Chapter 4[1]
Deep Space Station 13: Venus

The Venus site began operation in Goldstone, California, in 1962 as the Deep Space Network (DSN) research and development (R&D) station and is named for its first operational activity, a successful radar detection of the planet Venus. The 26-m Venus antenna was originally located at the Echo site (see Chapter 3 of this monograph), where it was erected to support Project Echo, an experiment that transmitted voice communications coast to coast by bouncing signals off the surface of a passive balloon-type satellite. In 1962, the antenna was moved, en masse, by truck, to its present location, a shielded site where research on and development of high-power transmitters could be carried out without causing radio interference at the other stations, and where the electromagnetic radiation danger to personnel could be minimized by the station layout. The Venus antenna is equipped with an azimuth-elevation-type mount. Its hydraulic drive system is designed for relatively fast angular movement and can be operated at 2 deg/s in elevation and azimuth. See Fig. 4-1 for a photograph of the Venus antenna in 1968.

The 2400-MHz planetary radar feed system configuration [1] is shown in Fig. 4-2. The Pioneer antenna, the Venus antenna, and all subsequent 26-m Cassegrain antennas were built with the same *F/D* ratio so that support cones could be interchangeable from one antenna to another. This cone interchangeability philosophy was used throughout the DSN for new antenna designs (the 64-m [2] and the 34-m high-efficiency [HEF] antennas) and has had an impact on the design parameters available for new designs. This philosophy was ulti-

[1]Based on "Evolution of the Deep Space Network 34-M Diameter Antennas," by William A. Imbriale, which appeared in *Proceedings of the IEEE Aerospace Conference*, Snowmass, Colorado, March 21–28, 1998. (© 1998 IEEE)

Fig. 4-1. DSS-13, the Venus antenna.

mately abandoned when beam-waveguide (BWG) antennas were introduced into the DSN.

The subreflector of the planetary radar feed system consists of a 96-in. (2.438-m)-diameter truncated hyperboloid with a 120-in. (3.048-m)-diameter nonoptical flange to reduce antenna noise temperature [3,4]. The flange is smaller than that of the 140-in. (3.556-m) Pioneer antenna system because of the higher frequency. A type of vertex plate and subreflector remote control similar to those of the Pioneer antenna were used.

A block diagram of the support-cone equipment is shown in Fig. 4-3. The polarizer is a turnstile-junction type [5]. This type of junction is a six-port device; two ports are spatially orthogonal (hybrid) H_{11} circular waveguide modes, two are H_{10} rectangular waveguide outputs, and the final two are short-circuit terminated H_{10} rectangular waveguide ports. By choosing the appropriate short-circuit lengths, it is possible to excite the feed horn with any type of polarization. Normally, circular polarization is used for radar experiments; two continuously rotatable spatially orthogonal modes of linear polarization may be obtained by manual change of the short circuits. The polarization switch allows remotely controlled selection of either right- or left-hand circular polarization, or two orthogonal linear polarizations.

As shown in Fig. 4-3, a second waveguide switch is used to switch the polarizer output either to the high-power transmitter or the receiving system. The third switch allows the receiver (maser) input to be switched between the

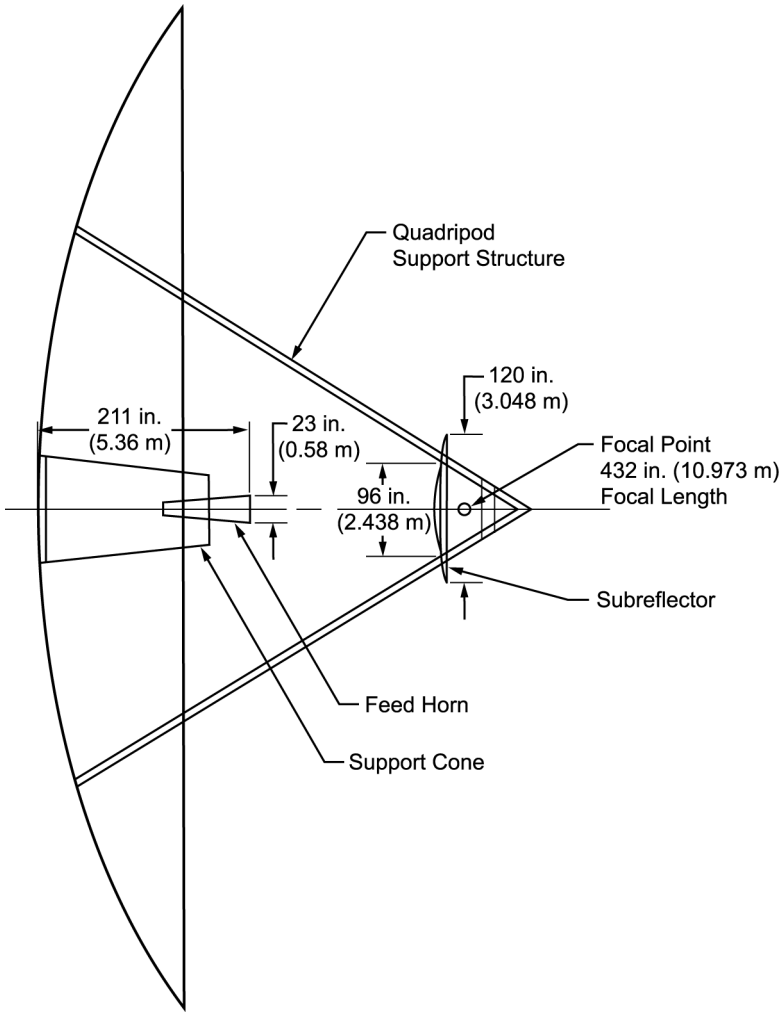

Fig. 4-2. Planetary radar antenna system.

antenna or either of two calibrating cryogenic terminations. During the normal transmit mode of radar operation, the polarization switch is in the right circular position, the transmit–receive switch is in the transmit position, and the calibration switch is in the nitrogen load position (the latter to provide additional isolation between transmitter output and receiver input). In the normal receiving configuration, the polarization and transmit–receive switch positions are reversed and the calibrate switch positioned to the antenna port. During radar operation, the transmitter drive and switch positions are changed remotely and automatically at time intervals that correspond to the round-trip propagation time between Earth and the planetary target.

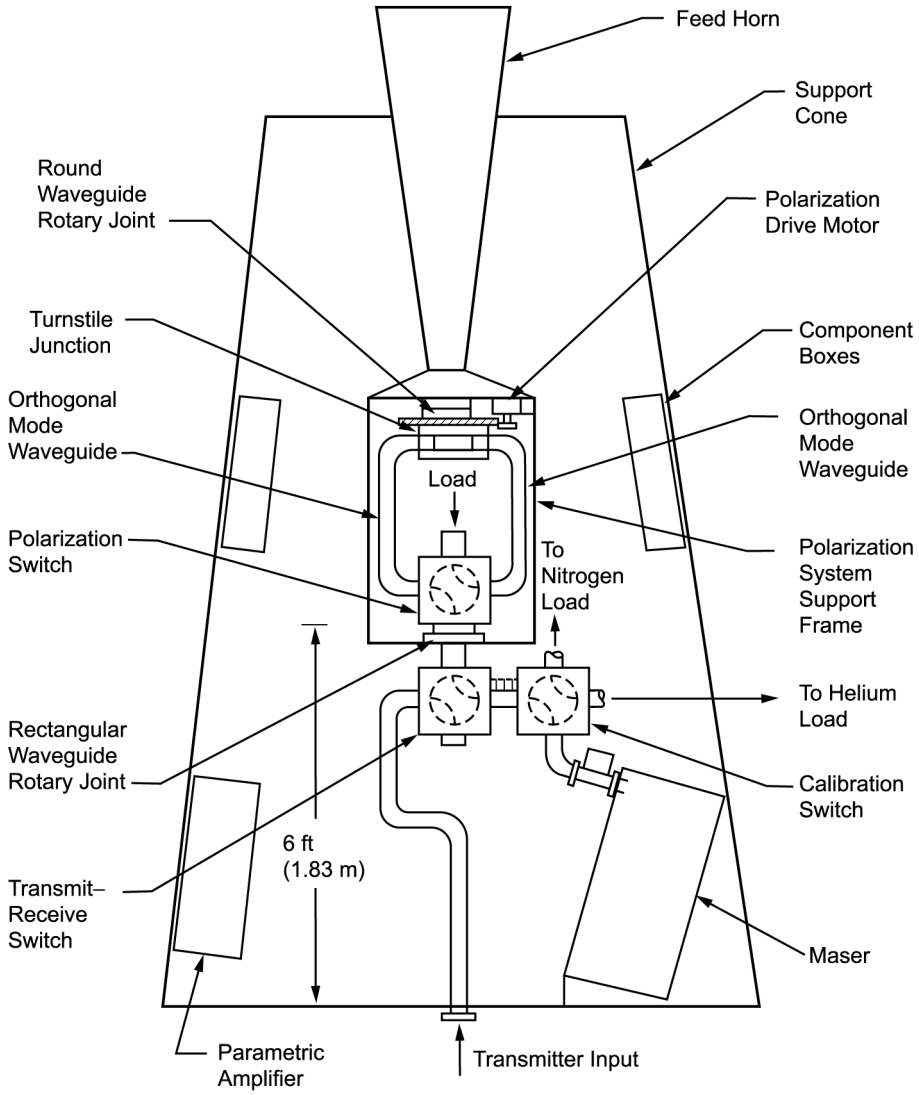

Fig. 4-3. Support-cone experiment layout.

The polarization flexibility and excellent axial ratio of the overall antenna system have been employed by Schuster and Levy [6,7] to perform a number of interesting polarization experiments with the planet Venus as a radar target.

4.1 The Dual-Mode Conical Feed Horn

The most significant improvement in the design of the Venus antenna was the change to a dual-mode conical feed horn [8,9], sometimes referred to as a Potter feed horn. It is well known that the conical feed horn, operating in the dominant circular (transverse-electric) TE_{11} mode, effectively has a tapered aperture distribution in the electric plane. For this reason, its beamwidths in the electric and magnetic planes are more nearly equal than those with a square pyramidal feed horn; this is a valuable feature for polarization diversity applications. An additional result of this tapered electric-plane distribution is a more favorable sidelobe structure than with the square feed horn. The dual-mode conical feed horn utilizes a conical feed horn excited at the throat region in both the dominant circular TE_{11} mode and the higher-order (transverse-magnetic) TM_{11} mode. These two modes are then excited in the feed-horn aperture with the appropriate relative amplitude and phase to effect complete beamwidth equalization in all planes, complete phase center coincidence, and at least 30-dB sidelobe suppression in the E-plane. Because of the desired presence of the higher-order TM_{11} mode in the feed horn, it is necessary to maintain extreme mechanical precision (of the order of 10^{-3} wavelength) on the inner surfaces to prevent mode conversion, with attendant pattern degradation. For this reason, very conservative mechanical design and fabrication techniques are used, and, as a result, the entire feed horn was machined from three solid aluminum billets.

4.2 Gain Calibration

The accurate gain calibration of large antenna systems poses a special problem because of the large distance involved in far-field tests (10.6 km for a 26-m [85-ft] antenna at 2.4 GHz). Consequently, a calibration signal source was installed on Mt. Tiefort, 20.4 km from the antenna. The technique used for gain calibration involved direct measurement of the signal attenuation between the antenna and the Mt. Tiefort signal source, using suitable corrections for atmospheric loss [10,11]. An accurate standard horn calibration of an identical dual-mode feed horn as the feed was performed, yielding an expected feed-horn gain value of 22.02 ± 0.09 dB. Using the above results, the 26-m antenna gain at the feed-horn output was found to be 54.40 ± 0.15 dBi; the corresponding aperture efficiency was 0.65. This was the most accurate gain measurement made on the 26-m antennas and was used for calibration of radio source absolute flux density.

A computer program was developed for secondary pattern and gain calculations, using feed radiation pattern data and calculated aperture blockage. The

quadripod was included in the calculation as four wedge-shaped regions corresponding to the physical outline of the trusswork with an opaqueness factor to account for the fact that trusswork is partially transparent. Table 4-1 compares the predicted and measured gain. The 63 percent opaqueness factor is the number derived from equating the measured and predicted gain. Table 4-1 indicates possibilities for future improvement. As was found in later developments, about a 1-dB improvement in performance was achieved by increasing the illumination efficiency by dual-reflector shaping and by decreasing effective quadripod blockage through more efficient structural design.

General techniques for determining effective antenna temperature have been derived by Schuster et al. [12]. The method used for evaluating the planetary radar system basically consists of comparing the noise power received by the antenna with that emitted by the liquid nitrogen and liquid helium terminations. Corrections for the small (0.1-dB) insertion losses in the various transmission paths were made, resulting in an overall standard deviation for the zenith antenna temperature of approximately 0.75 K. The mean value for the antenna temperature at the feed-horn output is 10.5 K. Figure 4-4 is a plot of the antenna temperature as a function of elevation angle, together with the temperature that would be observed if the only elevation angle dependence were that predicted by Hogg [10] for the atmosphere. Note that the forward sidelobe contribution to antenna noise temperature is scarcely discernible.

Table 4-1. Predicted and measured gain.

Item	Loss Factor (dB)	Associated Gain (dB)
Prediction factors		
Theoretical maximum gain	Not applicable	56.24
Illumination factor	–1.06	Not applicable
Gain for perfect surface and no quadripod	Not applicable	55.18
Surface tolerance loss (rms = 0.81 mm)	–0.05	Not applicable
Gain for no quadripod	Not applicable	55.13
Loss for 100 percent opaque quadripod (machine computed)	–1.19	Not applicable
Loss for 63 percent opaque quadripod	–0.73	Not applicable
Predicted gain for 63 percent opaque quadripod	Not applicable	54.40
Measured gain	Not applicable	54.50 ± 0.15

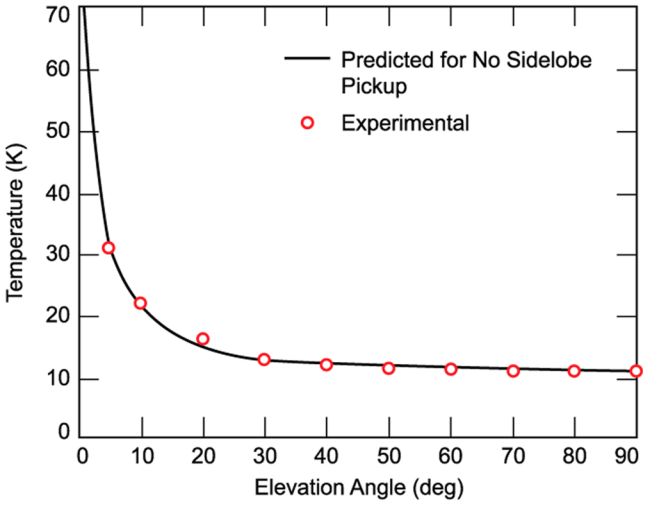

Fig. 4-4. Antenna temperature versus elevation angle.

Predicted and measured zenith antenna noise temperature performances are shown in Table 4-2; they demonstrate that zenith noise temperature may be predicted to good accuracy from a knowledge of the feed system patterns and the antenna physical characteristics.

The Venus antenna remained 26 m and was last equipped with the prototype common-aperture feed horn developed for the 34-m HEF antenna. With the advent of the new research and development 34-m BWG antenna built at the Venus site, the original 26-m antenna was removed from service.

Table 4-2. Predicted and measured zenith noise temperature.

Budget Elements	Predicted Values
Feed spillover (0.5%)	1.0 K (predicted from scale model tests)
Quadripod scattering	5.5 K (predicted from 9% blocking, energy assumed to scatter isotropically, averaged 240 K ground)
Surface leakage between panels	0.5 K (extrapolated from a measured value at a different frequency)
Atmosphere and extra atmospheric noise	3.0 K (measured)
	Totals
Predicted	10.0 K
Measured	10.5 ± 0.75 K standard deviation

References

[1] P. D. Potter, *The Design of a Very High Power, Very Low Noise Cassegrain Feed System for a Planetary Radar*, JPL TR 32-653, Jet Propulsion Laboratory, Pasadena, California, August 1964.

[2] Technical Staff, Tracking and Data Acquisition Organization, *The NASA/JPL 64-Meter-Diameter Antenna at Goldstone, California: Project Report*, JPL TM 33-671; Jet Propulsion Laboratory, Pasadena, California, July 1974.

[3] P. D. Potter, "Unique Feed System Improves Space Antennas," *Electronics*, vol. 35, pp. 36–40, June 1962.

[4] P. D. Potter, *A Simple Beamshaping Device for Cassegrainian Antennas*, JPL Technical Report TR 32-214; Jet Propulsion Laboratory, Pasadena, California, January 1962.

[5] R. S. Potter, "The Analysis and Matching of the Trimode Turnstile Waveguide Junction," NRL Report 4670, Naval Research Laboratory, Washington, D.C., December 1955.

[6] D. Schuster and G. S. Levy, "Faraday Rotation of Venus Radar Echoes," *Astronomical Journal*, vol. 69, no. 1, pp. 42–48, February 1964.

[7] G. S. Levy and D. Schuster, "Further Venus Radar Depolarization Experiments," *Astronomical Journal*, vol. 69, no. 1, pp. 29–33, February 1964.

[8] P. D. Potter, "A New Horn Antenna with Suppressed Sidelobes and Equal Beamwidth," *Microwave Journal*, vol. VI, no. 6, pp. 71–78, June 1963.

[9] P. D. Potter, and Ludwig, A. C., "Beamshaping by Use of Higher Order Modes in Conical Horns," *Nerem Record*, pp. 92–93, 1963.

[10] D. C. Hogg, "Effective Antenna Temperature Due to Oxygen and Water Vapor in the Atmosphere," *Journal of Applied Physics*, vol. 30, September 1959.

[11] J. H. Van Vleck, "Absorption of Microwaves by Oxygen," *Physical Review*, vol. 71, no. 6, pp. 413–433, March 1947.

[12] D. Schuster et al., "The Determination of Noise Temperature of Large Paraboloidal Antennas," *IRE Transactions on Antennas and Propagation*, vol. AP-10, no. 3, pp. 286–291, May 1962.